Mechanochemical preparation of chrysomycin A self-micelle solid dispersion with improved solubility and enhanced oral bioavailability

Zhuomin Xu
Zhejiang University of Technology
Shanshan Zheng
Zhejiang University of Technology
Yulu Hong
Zhejiang University of Technology
Yue Cai
Zhejiang University of Technology
Qiuqin Zhang
Zhejiang University of Technology
Jiani Xiang
Zhejiang University of Technology
Dehui Xie
Zhejiang University of Technology
Fuxing Song
Beijing Technology and Business University
Huawei Zhang
Zhejiang University of Technology
Hong Wang
Zhejiang University of Technology
Xuanrong Sun (sunxr@zjut.edu.cn)
Zhejiang University of Technology https://orcid.org/0000-0001-5414-9300

Research

Keywords: Chrysomycin A, mechanochemistry, ball milling, solid dispersion, self-micelle, bioavailability, antitumor

Posted Date: March 13th, 2021

DOI: https://doi.org/10.21203/rs.3.rs-286030/v1

Abstract

Background: Chrysomycin A (CA) has been reported as numerous excellent biological activities, such as antineoplastic and antibacterial. Though, poor solubility of CA limited its application in medical field. Due to good amphiphilicity and potential anticancer effect of disodium glycyrrhizin (Na_2GA) as an excipient, an amorphous solid dispersion (Na_2GA/CA-BM) consisting of CA and Na_2GA was prepared in the present study by mechanochemical technology (roll mill ML-007, zirconium balls, 30 rpm, 2.5 h) to improve the solubility and oral bioavailability of CA. Then, Na_2GA/CA-BM was self-assembled to micelles in water. The interaction of CA and Na_2GA in solid state were investigated by X-ray diffraction studies, polarized light microscopy, and scanning electron microscope. Meanwhile, the properties of the sample solution were analyzed by dynamic light scattering and transmission electron. Furthermore, the oral bioavailability and antitumor ability of Na_2GA/CA-BM in vivo were tested, providing a theoretical basis for future application of CA on cancer therapy.

Results: CA encapsulated by Na_2GA was self-assembled to nano-micelles in water. The average diameter of nano-micelle was 131.6 nm, and zeta potential was -11.7 mV. Three physicochemical detections showed that CA was transformed from crystal into amorphous form after treated with ball milling and the solubility increased by 50 times. Na2GA/CA-BM showed a significant increase of the bioavailability about 2 time that of free CA. Compared with free CA, the in-vivo antitumor studies also exhibited that Na_2GA/CA-BM had an excellent inhibition of tumor growth.

Conclusions: Na_2GA/CA-BM nanoparticles (131.6 nm, -11.7 mV) prepared by simple and low-cost mechanochemical technology can improve oral bioavailability and antitumor efficacy of CA in vivo, suggesting a potential formulation for efficient anticancer treatment.

Introduction

Chrysomycins is a novel antibiotic complex isolated from *Streptomyces* spp, containing compounds of C-glycosides antitumor actives [1]. Especially, Chrysomycin A (CA, Fig. 1) is the major analogue of chrysomycins and plays the most potent role in this complex [2]. Compared with the clinically used anticancer agent doxorubicin, CA shows significant cytotoxicity toward cancer cells because of its vinyl group in the 8-position [3, 4]. In addition to strong antineoplastic and antibacterial properties of CA [5–7], it is thought to act as an inhibitor of the catalytic activity of human topoisomerase □ [8]. Besides, CA equips with strong antifungal profile, and its cytotoxicity to normal cells can be negligible. Meanwhile, it has no effect on the lysis of red blood cells [6]. All these characteristics indicate that CA has the potential to be a good anti-tumor, anti-bacterial and even anti-fungal candidate. Nonetheless, the oral bioavailability of CA is low owe to its poor solubility in water, which restricts its clinical application. To the best of our knowledge, there are no studies on how to overcome these shortcomings of CA.

Generally, several approaches were employed to improve drug insolubility and bioavailability, such as preparation of polymeric micelles [9, 10], cyclodextrins inclusion complex [11, 12], solid dispersions (SDs)

[13, 14], self-emulsifying drug delivery system [15], and so on. In the methods mentioned above, most of need multiple organic solvents (e.g. dimethyl sulfoxide, N,N-dimethylformamide, dichloromethane, etc.), large quantity of surfactants, complex procedures, long preparation time, or expensive excipients (including cholesterol, lipids) [16]. Those are considered unfriendly to the environment, and may increase the risk of solvent exposure during preparation and the cost of production.

Mechanochemical technology has become extensively popular in the field of pharmaceutical sciences for its important role in the development of green synthesis [17, 18], cocrystal synthesis [19, 20], and amorphous SDs [21, 22]. When the high intensity of mechanical energy is transferred to the solid state substances, the strain is generated and may cause plastic deformation and concurrent changes in the crystal structure along with crystalline phase transitions and amorphization [23]. All the changes may potently enhance the solubility and bioavailability [24]. Compared with traditional “liquid phase” way, mechanochemical treatment provides significant advantages such as one-step technological process, absence of solvents, and low operating cost.

Disodium glycyrrhizinate (Na_2GA) is the salt formation of glycyrrhizic acid (GA), which can undergo hydrolysis in aqueous solutions and generated free GA. As for GA, it is a good soluble natural saponin, having antiviral[25], anti-inflammatory[26] and anticancer[27] properties. Apart from those features, GA forms non-covalent compounds with various drugs due to its amphiphilicity. Such supramolecular compounds could increase the solubility of hydrophobic drugs up to dozens of times, and enhance the permeability of drug through cell membranes[28–30]. In contrast, Na_2GA solution is lower viscosity and more environment-friendly than GA solution. Meanwhile, Na_2GA also been reported to have antitumor activity. Zhang et al. formed an amorphous SD of curcumin and Na_2GA utilizing mechanochemistry to enhance the bioavailability and cytotoxic activity of curcumin. Zhu et al. encapsulated SN-38 into Na_2GA for preparing a SN-38 self-micelle SD resulting in markly improving the solubility and antitumor activity of SN-38.

Given that mechanochemical technology and Na_2GA have the potential to improve the solubility and bioavailability of water insoluble drug, in this study, solid dispersion of CA were prepared mechanical milling with Na_2GA. The physical characteristics, solubility, pharmacokinetics, tissue distribution and anti-tumor activity of CA as an amorphous SD were further investigated.

Materials And Method

Materials

CA was obtained from professor Song Fuxing (Beijing Technology and Business University, purity >99%). Disodium salt of glycyrrhizic acid (Na_2GA) was purchased from Shanxi Pioneer Biotech Co. Ltd. (Xian, China, purity >98%). Acetonitrile was obtained from Tedia Company, Inc. (Fairfield, OH, USA, HPLC grade). Formic acid with purity >88% was purchased from Aladdin Bio-Chem Technology Co., Ltd. (Shanghai,

China). Roswell Park Memorial Institute 1640 (RPMI-1640) cell culture medium, fetal bovine serum (FBS) and penicillin/ streptomycin were all purchased from Gibco BRL (Gaithersburg, MD, USA).

Cells and animals

The mouse melanoma cell line B16-F10 was purchased from the China Center for Type Culture Collection (Wuhan, China) and cultured in RPMI-1640 containing 10% FBS and 1% antibiotics (penicillin/ streptomycin).

Female ICR mice (5-6 weeks of age, 18-20 g body weight) and female C57BL/6 mice (5 to 6 weeks of age, 16-18g) used in the experiments were provided by the Zhejiang Academy of medical Science, conducting with the approval of the animal experiment center of Zhejiang University of Technology. All the animals were performed in strict compliance with the PR China legislation for the use and care of laboratory animals.

Fabrication of nanoparticles by mechanochemical treatment

The roll mill ML-007 (Wiggens, German) was used to prepare samples. Briefly, 0.15 g CA and 14.85 g Na_2GA (weight ratio 1/99) were added to 300 mL vial with 660.0 g zirconium balls (diameter 22 mm) with milling time of 3 h, rotation speed 30 rpm and samples were picked out at 0.5, 1, 1.5, 2, 2.5 h, and 3 h, respectively. In addition, a mixture of Na_2GA and CA (weight ratio was same as above) by ordinary physical treating without ball milling, were prepared for comparing with the ball milling products. At last, the ball-milling products with different milling time were described as BM-0.5 h, BM-1.0 h, BM-1.5 h, BM-2.0 h, BM-2.5 h, BM-3 h, and the physical milling product was described as Na_2GA/CA-PM.

Analysis of chrysomycin A by HPLC

The appropriate amounts of samples were dissolved completely in a mixture solution (deionized water to acetonitrile, 1:1, v/v) respectively, and filtered through a 0.22 μm filter paper. Then, the filterate was determined by a high performance liquid chromatography (HPLC, Aglient 1260 infinity Ⅱ) equipped with column Inertisil O DS-3 C_{18} (250 mm×4.6 mm, 5 μm, GL Science Inc., Japan) at 25 ℃, and a UV detector set at a wavelength of 254 nm. Acetonitrile-0.1%formate water (40:60) was used as eluent (pH=2.6-2.8) with the flow rate of 1.0 ml/min.

Solubility determination

To determine the solubility, an overdose of samples and CA, were put into 500 μL of deionized water respectively and stirred for 12 h at 25 ℃. Finally, these solutions were filtered and analyzed by HPLC.

Powder X-ray diffraction (XRD)

X-ray diffraction test of samples was implemented with a Bruker D_2 Phase diffractometer (Buker, Germany) by using CuKα radiation. Step range: 3°-40°. Counter speed: 3.7°/min. All the data were

analyzed through GraphPad Prism 7.

Polarized light microscopy (PLM)

To distinguish the refraction phenomenon of samples, a small amount of solid powder was placed on microscope slide and observed by an Olympus CX41 polarized microscope (Japan) with a CCD camera (HTC1600, China). All the pictures were obtained at 10× resolution.

Scanning electron microscopy (SEM)

After samples were coated with platinum by a Leica EM ACE200 Vacuum Coater (Germany), SEM (ZEISS Gemini500, Germany) was performed to acquire electronic images. The Coating parameter: amperage 30 mA, spraying time 100 s.

Particle characterization and zeta potential

The physicochemical properties of samples containing hydrodynamic diameter, polydispersity index (PDI), and zeta potential, were detected using dynamic light scattering (DLS) instrument (Zetasizer NanoZS, Malvern Instruments, Malvern, UK) at 25 ℃. Before being measured, all samples were dissolved in deionized water at the concentration of 1 mg/mL, then filtered by a 0.22 μm filter.

Transmission electron microscopy (TEM)

To observe the morphology of micelle, samples were configured into 1mg/ml solution. One drop of sample was dripped on a carbon Formvar-coated cooper grid for a minute, and then were dried below the infrared light. Finally, TEM (Hitachi HT700 EXALENS, Japan) was at a working voltage of 100 kV to form the morphology of samples.

Pharmacokinetic evaluation

Ten female ICR mice were randomly divided into two groups (CA and the ball-milling produc to evaluate the pharmacokinetic of samples. The samples were dispersed in deionized water and were intragastriclly administered to the mice at the equivalent dose of 50mg/kg CA. Next, 0.2 mL of blood was collected into prepared heparinized tubes at different time points (0.25, 0.5, 1, 2, 4, 8, 12, and 24 h) after administration, and then centrifuged at 5,000 rpm, 4 ℃ for 5 minutes to obtain plasma supernatant. After taking plasma to a cleaning tube, a certain volume of acetonitrile was added to the supernatant (the volume ratio was 3:1). When protein precipitates generated, the mixture was vortexed for 2 minutes, and centrifugated at 10,000 rpm, 4 ℃ for 10 minutes. Then, supernatant from the mixture was extracted and stored at -80 ℃ for 2 h for furth use. After being thawed, samples were centrifugated (10,000 rpm, 4 ℃) for 10 minutes and take out. At last, the sample was filtered by a 0.22 μm filter for HPLC analysis.

In vivo tissue biodistribution study

To investigate the tissue biodistribution of CA and the ball-milling product, ten female ICR mice were stochastically divided into two groups. The ball-milling sample and CA were formulated as suspensions at a concentration of 5 mg/mL. The dose for each intragastric administration was 50 mg/kg equivalent to the concentration of CA. At the set time points (2 h, 6 h, 12 h), major organs containing heart, liver, spleen, lung, kidney, brain, skeletal muscle were resected and wash with 10mM phosphate buffered saline (PBS). After being dried and weighted, the organs were divided into small pieces and homogenized with deionized water at ratio of 1:2 (g /mL). To extract CA from tissues, the homogenate was added with acetonitrile (the ratio was 1:3). Then the mixture was vortexed for 1 minutes and centrifuged at 10,000 rpm, 4 ℃ for 10 minutes. Ultimately, supernatant was removed from the mixture to a clean tube and stored at -80 ℃ for HPLC analysis.

In vivo antitumor efficacy

The tumor-bearing model was established by subcutaneously injecting 1×10^6 B16-F10 cells in 100μL of PBS into female C57BL/6 mice at the right flank. When the tumor volume reached to about 35-60 mm^3, the mice were casually divided into 3 groups (n= 6 /group). Each mouse was intragastrically administered with an equivalent dose of 50mg/kg CA every 2-3 days, whereas the control group was given PBS.

The tumor growth and body weight change were monitored every 2-3 days. The tumor volume was measured with a caliper and was calculated as follows: tumor volume = $0.5\times length\times width^2$. On the 12th day, the mice were sacrificed, then the tumor and major organs (hearts, lungs, livers, kidneys and spleens) were washed with PBS and weighed. Moreover, tumor paraffin sections of three groups were stained with H&E staining to observe pathological changes.

Statistical analysis

Data were reported as mean±standard error of the mean, using the unpaired Student's *t*-test. Values of $*p < 0.05$ and $***p < 0.001$ calculated by GraphPad Prism 7 were considered significant and extremely significant, respectively.

Results And Discussion

Solubility determination of chrysomycin A SDs

The solubility of CA and its ball milling products was shown in Table 1. It could be seen that there were significant differences between CA (1.68 ± 0.66 μg/mL) and the SD samples. In addition, the solubility of CA SDs was gradually increased by prolonging the ball milling time from 0.5 to 2.5 hours. The drug milled for long time provided better wettability and dispersibility which was formed as the amorphous complex and encapsulated in a hydrophilic carrier. The solubility of Na_2GA/CA SD was excellently raised after the formation. However, an unwanting decreased of the solubility could be observed after milling for 3 hours. It was supposed that further aggregation of the particles resulting in their higher surface energy with

increased time of milling process, and thereby decreasing the solubility[31]. Since the sample created by ball milling for 2.5 hours had the best solubility (82.41±25.32 μg/mL) which was increased about 50 times compared with unprocessed pure CA, it was chose as chrysomycin A SDs candidate to study the subsequent experiments and was described as Na_2GA/CA-BM.

Physicochemical changes of chrysomycin A SDs

Physicochemical changes were analyzed by XRD, PLM and SEM. The X-ray diffractograms of CA, Na_2GA, Na_2GA/CA-Pand Na_2GA/CA-BM are shown in Figure 2a. CA displayed several sharp peaks at diffraction angles (2θ) of 6.67, 7.50, 9.47, 15.09, 21.60, indicating its crystalline form. On the other hand, the characteristic peaks of CA existed in the mechanical treated sample indicating it was still a crystal form. However, the crystallization peaks of CA were markedly decreased in the diffraction spectrum of Na_2GA/CA-PM, and even no characteristic peaks were observed in the sample of Na_2GA/CA-BM. The phenomenon could be attributed to the completely loss of crystalline of CA owing to high-intensity ball milling process. These XRD results further confirmed that CA which was dispersed in excipient Na_2GA to form an amorphous complex by ball milling.

The micrographs of CA, Na_2GA, Na_2GA/CA-PM and Na_2GA/CA-BM obtained from polarized light microscopy are shown in Figure 2b. As observed in the unprocessed CA, there was extensive birefringence, confirming its crystalline nature. In the Na_2GA/CA-PM micrograph of the physical mixture, the birefringence of CA was dispersed partially. After mechanochemical treatment, Na_2GA/CA-BM was shown no birefringence which identified the amorphous nature of CA embedded in Na_2GA.

Furthermore, the electron micrographs of CA, Na_2GA, Na_2GA/CA-PM and Na_2GA/CA-BM are shown in Figure 2c. It could be clearly seen that pure CA was elongated solid and the Na_2GA was composed of hollow spherical particle with a smooth surface texture. On the contrary, the intact morphology of CA and Na_2GA were disappeared and showed a fine and irregularly shaped particle for the ball-milling product Na_2GA/CA-BM, suggesting the amorphous solid phase structure of Na_2GA/CA-BM. The most noteworthy, that the noted particles dispersed more uniformly after being ground for 2.5 hours, possibly increased its surface thus improving the velocity of dissolution.

Properties of chrysomycin A micelles in water solution

When the Na_2GA/CA-BM dissolved in water, Na_2GA coated CA to form CA micelles. The size, zeta potential and surface morphology of micelles are all crucial for interactions between the cell membranes and micelles. As shown in Figure 3a, the average diameter of the particle was about 131.6 nm with a narrow size distribution at 25°C, and its polymer dispersity index (PDI) value was about 0.230. Moreover, the particle has a negative zeta potential which was -11.7 mV. It was reported that suitable range of particle sizes for evading filtration in reticuloendothelial system (RES) organs was between 100 and 200 nm. In addition, the neutral surface charge of particles (zeta potential ± 10mV) was proved to prolonged blood circulation and facilitate its accumulation at the tumor tissue[32]. Therefore, Na_2GA/CA-BM formed

a great candiate to further use in the animal studies due to proper diameter and potential. Furthermore, the images of micelle appearance observed by TEM are depicted in Figure 3b. The nano-micelle was spherical with smooth boundaries. The diameter of nano-micelle was about 100nm and slightly smaller than DLS data because of its shrinkage when dried before TEM detection.

Pharmacokinetic evaluation

The concentration-time curves of CA in mice plasma are depicted in Figure 4a, and the pharmacokinetic parameters are summarized in Table 2. From the figure, it could be clearly seen that the bioavailability of Na_2GA/CA-BM was improved than pure CA. After intragastric administration, CA and Na_2GA/CA-BM both distributed rapidly and reached the max blood concentration at 0.5 hour. What's more, the accumulation time in the body of Na_2GA/CA-BM was longer about 2-fold than the retention time of free CA. Then, the free CA was cleared faster from blood than Na_2GA/CA-BM, so Na_2GA/CA-BM had a better blood circulation in the body. Compared with CA, the area under the curve of Na_2GA/CA-BM was increased about 1.8 times larger, and the plasma clearance was dramatically decreased.

Tissue distribution study

Figure 4b depicts the distribution concentration of CA in major tissues of mice including heart, liver, spleen, lung, kidney, brain, skeletal muscle after oral dose of 50mg/kg of either Na_2GA/CA-BM or CA. After intragastric administration for 2h, the concentration of CA (Na_2GA/CA-BM group) was high in spleen, and reached to the highest blood concentration at 6h, after that CA gradually cleared and finally expelled at about 12h. As for free CA group, CA was distributed mainly in spleen, liver, lung, kidney and muscle, and slowly cleared after 12 hours. The main metabolic organ of CA was liver and spleen, while Na_2GA/CA-BM was metabolized mainly in spleen after 6 hours. Generally, large size of particles were preferentially absorbed by the liver, and small particles were easily cleared by the spleen, which led to the change in metabolic site of drug. In comparison, Na_2GA/CA-BM showed longer blood accumulation in body than free CA after 12h, which was consistent with the results of the pharmacokinetic study.

In vivo antitumor efficacy

Due to the better performance on the solubility and bioavailability, we next evaluated the antitumor ability of Na_2GA/CA-BM on B16-F10 tumor-bearing C57BL/6 mice. As shown in Figure 5a, CA and Na_2GA/CA-BM both inhibited the growth of B16-F10 tumors compared with the control group. Meanwhile, Na_2GA/CA-BM showed better tumor suppression ability throughout the treatment, and the tumor inhibition rate was closed 40.1%. From Figure 5b, it was found that none of the mice loss body weight obviously after treating CA formulations, which indicated no potential systemic toxicities of CA and Na_2GA/CA-BM.

After tumors excision, the weights (Figure 5c) of tumors treated with Na_2GA/CA-BM (1.800±1.246 g) were lower than those of the mice treated with CA (2.230±1.429 g) or PBS (2.212±1.192 g). In addition, the

tumor weights of CA group showed no significant differences compared with the control group.

H&E staining were shown to observe pathological changes of tumor cells in three groups, As shown in Figure 5d, the tumor cells were dense and had abundant vascular tissue in all three groups. Karyopycnosis and deep staining could be seen, which meant apoptosis and necrosis of cancer cells. Thus, different degrees of apoptosis were seen in tumors treated with CA and Na_2GA/CA-BM. In comparison, a large amount of excessive vacuolization and more apoptosis cells were observed in the tissue section of Na_2GA/CA-BM group. Moreover, various size tumor cells could be seen in the envelop layer of tumor tissue treated with PBS and the free CA, rather than in tumor layer of Na_2GA/CA-BM group, indicating the excellent antitumor ability of Na_2GA/CA-BM.

Conclusions

In the present study, an amorphous CA solid dispersion was successfully prepared by mechanical ball milling. As compared to the free CA, Na_2GA/CA-BM exhibited superior solubility evidenced by a about 50-fold increase. The physicochemical characteristics analysis showed that CA was dispersed uniformly in the hydrophilic carrier (Na_2GA) and transformed from crystals into amorphous state by ball milling. When Na_2GA/CA-BM dissolved in water, CA encapsulated by Na_2GA was self-formed to micelles. Consistent with the amorphous nature and self-formed micelles of Na_2GA/CA-BM, it showed significant improvement of pharmacokinetic behavior in mice, which increased 1.8 times in oral bioavailability. Moreover, Na_2GA/CA-BM also exhibited a stronger antitumor ability than CA due to the improvement of oral bioavailability. In summary, our work illustrated an unprecedented and environment-friendly preparation of the CA formulation by ball milling approach, which are promising to enhance the oral bioavailability and antitumor ability of CA, might be considered for efficient anticancer therapy.

Declarations

Acknowledgements

This work was supported by grants from the National Key R&D Program of China (2018YFC0311005), the National Natural Science Foundation of China (No. 22075247), and the Zhejiang Provincial Natural Science Foundation of China (No. LGF21C100001), Research Foundation for Advanced Talents of Beijing Technology and Business University (No. 19008020158).

Authors' contribution

XS, HZ and HW conceived and designed the experiments. FS provided chrysomycin A. ZX, CY, SZ, and YH performed experiments. QZ and JX provided technical support for the preparation of Na_2GA/CA-BM, DX provided technical support for the antitumor activity. ZX analyzed data and wrote the article. XS interpreted data and reviewed the manuscript. All authors read and approved the final manuscript.

Availability of data and materials

The datasets used and/or analysed during the current study are available from the corresponding author on reasonable request.

Ethics approval and consent to participate

All experimental procedures involving animals performed in this study were previously approved and certified (NO.20200824109) by the animal experiment center of Zhejiang University of Technology, which performed in strict compliance with the PR China legislation for the use and care of laboratory animals.

Consent for publication

Not applicable.

Competing interests

The authors declare that they have no competing interests.

References

1. Matson JA, Rose WC, Bush JA, Myllymaki R, Bradner WT, Doyle TW. Antitumor activity of chrysomycins M and V. J Antibiot. 1989;42:1446–8.
2. Weiss U, Yoshihira K, Highet RJ, White RJ, Wei TT. The chemistry of the antibiotics chrysomycin A and B. Antitumor activity of chrysomycin A. J Antibiot. 1982;35:1194–201.
3. Li Y, Huang X, Ishida K, Maier A, Kelter G, Jiang Y, Peschel G, Menzel K, Li M, Wen M, Xu L, Grabley S, Fiebig H, Jiang C, Hertweck C, Sattler I. Plasticity in gilvocarcin-type C-glycoside pathways: Discovery and antitumoral evaluation of polycarcin V from Streptomyces polyformus. Org Biomol Chem. 2008;6:3601–5.
4. Wada S, Sawa R, Iwanami F, Nagayoshi M, Kubota Y, Iijima K, Hayashi C, Shibuya Y, Hatano M, Igarashi M, Kawada M. Structures and biological activities of novel 4 '-acetylated analogs of chrysomycins A and B. J Antibiot. 2017;70:1150.
5. Kudinova MK, Kuliaeva VV, Potapova NP, Rubasheva LM, Maksimova TS. Separation and characteristics of the components of the antibiotic virenomycin. Antibiotiki. 1982;27:507–11.
6. Muralikrishnan B, Dan VM, Vinodh JS, Jamsheena V, Ramachandran R, Thomas S, Dastager SG, Kumar KS, Lankalapalli RS, Kumar RA. Anti-microbial activity of chrysomycin a produced by Streptomyces sp. Against Mycobacterium tuberculosis. Rsc Adv. 2017;7:36335–9.
7. Jain SK, Pathania AS, Parshad R, Raina C, Ali A, Gupta AP, Kushwaha M, Aravinda S, Bhushan S, Bharate SB, Vishwakarma RA. Chrysomycins A-C, antileukemic naphthocoumarins from Streptomyces sporoverrucosus. Rsc Adv. 2013;3:21046–53.

8. Lorico A, Long BH. Biochemical characterisation of elsamicin and other coumarin-related antitumour agents as potent inhibitors of human topoisomerase II. European journal of cancer. 1993;29A:1985–91.
9. Gu Q, Xing JZ, Huang M, He C, Chen J. SN-38 loaded polymeric micelles to enhance cancer therapy. Nanotechnology. 2012;23:1–10.
10. Liu Y, Yang G, Baby T, Tengjisi, Chen D, Weitz DA, Zhao C. Stable polymer nanoparticles with exceptionally high drug loading by sequential nanoprecipitation. Angew Chem Int Edit. 2020;59:4720–8.
11. Hammoud Z, Khreich N, Auezova L, Fourmentin S, Elaissari A, Greige-Gerges H. Cyclodextrin-membrane interaction in drug delivery and membrane structure maintenance. Int J Pharmaceut. 2019;564:59–76.
12. Terauchi M, Inada T, Tonegawa A, Tamura A, Yamaguchi S, Harada K, Yui N. Supramolecular inclusion complexation of simvastatin with methylated beta-cyclodextrins for promoting osteogenic differentiation. Int J Biol Macromol. 2016;93:1492–8.
13. Javeer SD, Patole R, Amin P. Enhanced solubility and dissolution of simvastatin by HPMC-based solid dispersions prepared by hot melt extrusion and spray-drying method. Journal of Pharmaceutical Investigation. 2013;43:471–80.
14. Wang F, Xiao X, Yuan Y, Liu J, Liu Y, Yi X. Solubilization of phloretin via steviol glycoside-based solid dispersion and micelles. Food Chem. 2020;308:125569.
15. Saggar S, Upadhayay A, Goswami M. Formulation and evaluation of solid self-emulsifying drug delivery system of bambuterol hydrochloride. Indian J Pharm Sci. 2019;81:661–72.
16. Zhang Q, Polyakov NE, Chistyachenko YS, Khvostov MV, Frolova TS, Tolstikova TG, Dushkin AV, Su W. Preparation of curcumin self-micelle solid dispersion with enhanced bioavailability and cytotoxic activity by mechanochemistry. Drug Deliv. 2018;25:198–209.
17. Bahri M, Kazemian H, Rohani S, Haghighat F. Mechanochemical synthesis of CPM-5: A green method. Chem Eng Technol. 2017;40:88–93.
18. Wei G, Li Y, Zhang L, Cai S, Zhu T, Li Z, Mo J. Synthesis of bentonite-supported Fe(II) and heteropolyacid (HPW) composite through a mechanochemical processing. Appl Clay Sci. 2018;152:342–51.
19. Da Silva CCP, de Melo CC, Souza MS, Diniz LF, Carneiro RL, Ellena J. 5-Fluorocytosine/5-Fluorouracil Drug-Drug cocrystal: A new development route based on mechanochemical synthesis. J Pharm Innov. 2019;14:50–6.
20. Douroumis D, Ross SA, Nokhodchi A. Advanced methodologies for cocrystal synthesis. Adv Drug Deliver Rev. 2017;117:178–95.
21. Xu W, Wen M, Yu J, Zhang Q, Polyakov NE, Dushkin AV, Su W. Mechanochemical preparation of kaempferol intermolecular complexes for enhancing the solubility and bioavailability. Drug Dev Ind Pharm. 2018;44:1924–32.

22. Sun X, Zhu D, Cai Y, Shi G, Gao M, Zheng M. One-step mechanochemical preparation and prominent antitumor activity of SN-38 self-micelle solid dispersion. Int J Nanomed. 2019;14:2115–26.
23. Boldyrev VV. Mechanochemical modification and synthesis of drugs. J Mater Sci. 2004;39:5117–20.
24. Descamps M, Willart JF. Perspectives on the amorphisation/milling relationship in pharmaceutical materials. Adv Drug Deliver Rev. 2016;100:51–66.
25. Pompei R, Laconi S, Ingianni A. Antiviral properties of glycyrrhizic acid and its semisynthetic derivatives. Mini-Rev Med Chem. 2009;9:996–1001.
26. Bernela M, Ahuja M, Thakur R. Enhancement of anti-inflammatory activity of glycyrrhizic acid by encapsulation in chitosan-katira gum nanoparticles. Eur J Pharm Biopharm. 2016;105:141–7.
27. Su X, Wu L, Hu M, Dong W, Xu M, Zhang P. Glycyrrhizic acid: A promising carrier material for anticancer therapy. Biomed Pharmacother. 2017;95:670–8.
28. Yang F, Zhang Q, Liang Q, Wang S, Zhao B, Wang Y, Cai Y, Li G. Bioavailability enhancement of paclitaxel via a novel oral drug delivery system: Paclitaxel-Loaded glycyrrhizic acid micelles. Molecules. 2015;20:4337–56.
29. Kong R, Zhu X, Meteleva ES, Chistyachenko YS, Suntsova LP, Polyakov NE, Khvostov MV, Baev DS, Tolstikova TG, Yu J, Dushkin AV, Su W. Enhanced solubility and bioavailability of simvastatin by mechanochemically obtained complexes. Int J Pharmaceut. 2017;534:108–18.
30. Selyutina OY, Polyakov NE, Korneev DV, Zaitsev BN. Influence of glycyrrhizin on permeability and elasticity of cell membrane: Perspectives for drugs delivery. Drug Deliv. 2016;23:858–65.
31. Du L, Dushkin AV, Chistyachenko YS, Polyakov NE, Su W. Investigation the inclusion complexes of valsartan with polysaccharide arabinogalactan from larch Larix sibirica and (2-hydroxypropyl)-beta-cyclodextrin: Preparation, characterization and physicochemical properties. J Incl Phenom Macro. 2016;85:93–104.
32. Li S, Huang L. Pharmacokinetics and biodistribution of nanoparticles. Mol Pharmaceut. 2008;5:496–504.

Figures

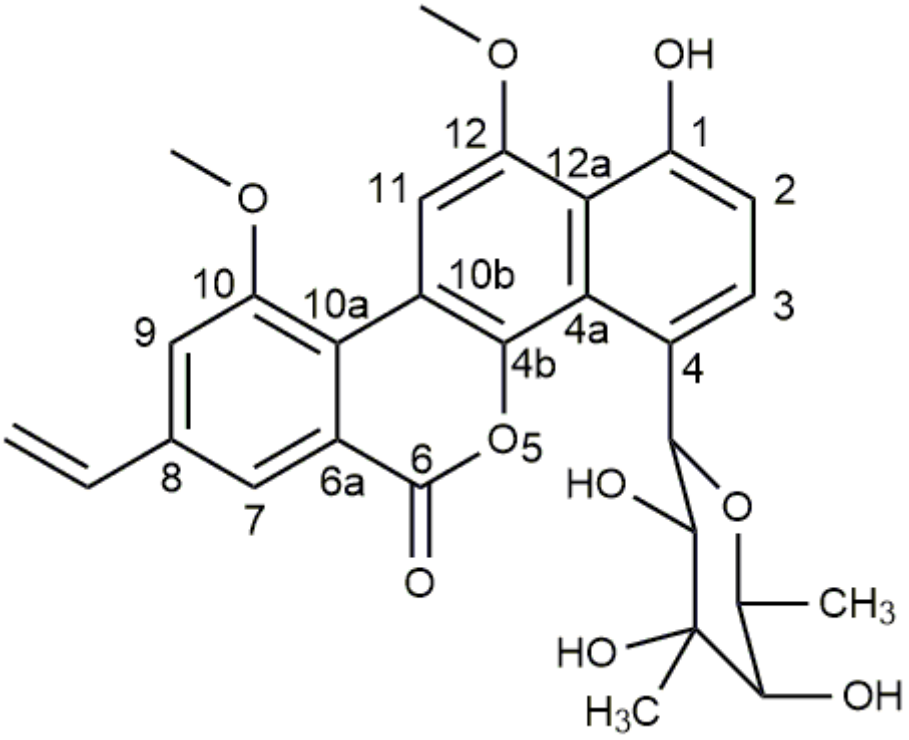

Figure 1

Chemical structure of chrysomycin A

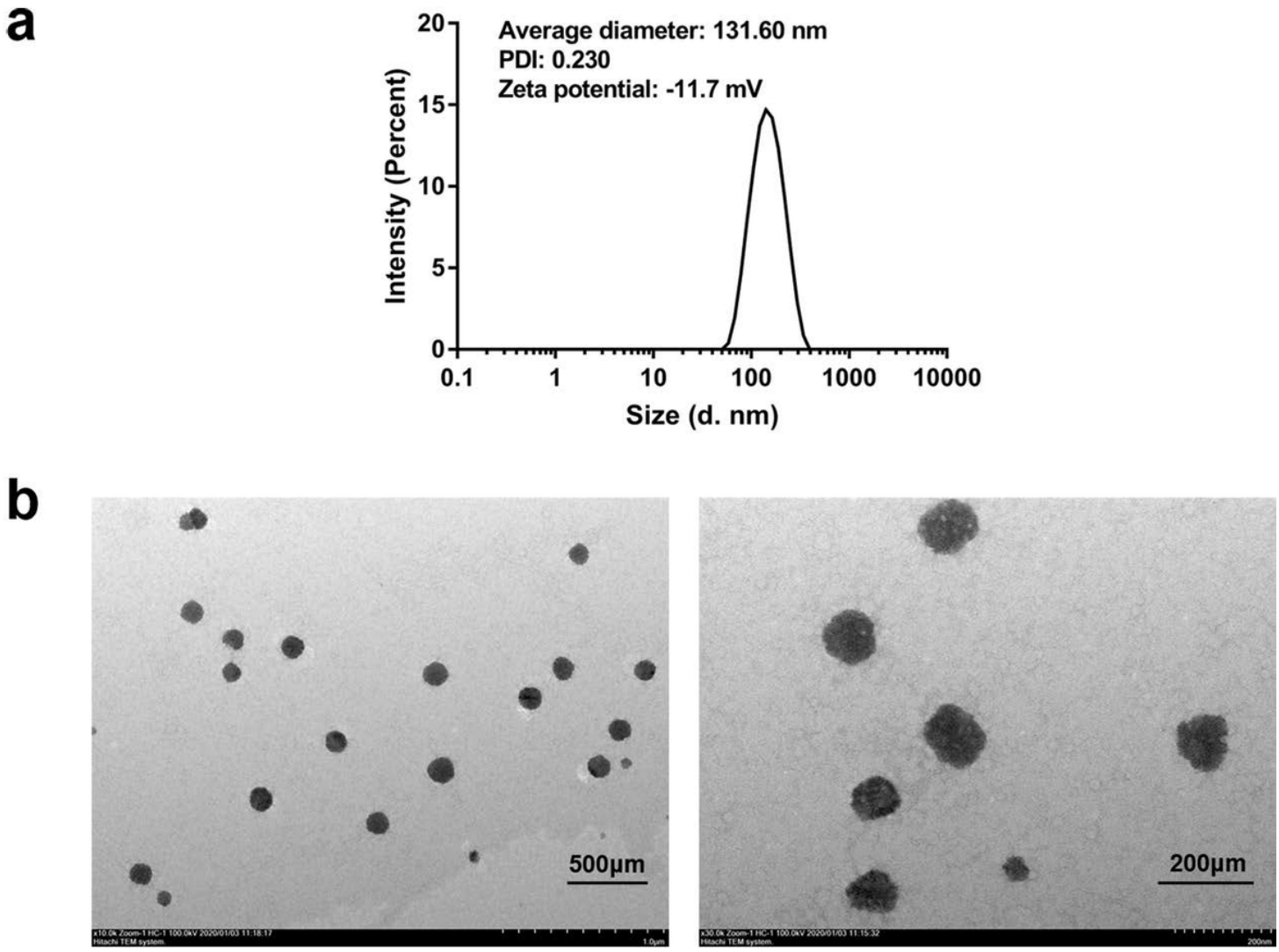

Figure 2

(a) X-ray diffraction spectra of CA, Na2GA, Na2GA/ CA-PM, Na2GA/ CA-BM. (b) PLM images of CA, Na2GA, Na2GA/CA-PM, Na2GA/CA-BM, the magnification was 10×. (c) The electron micrographs of CA, Na2GA, Na2GA/CA-PM, Na2GA/CA-BM.

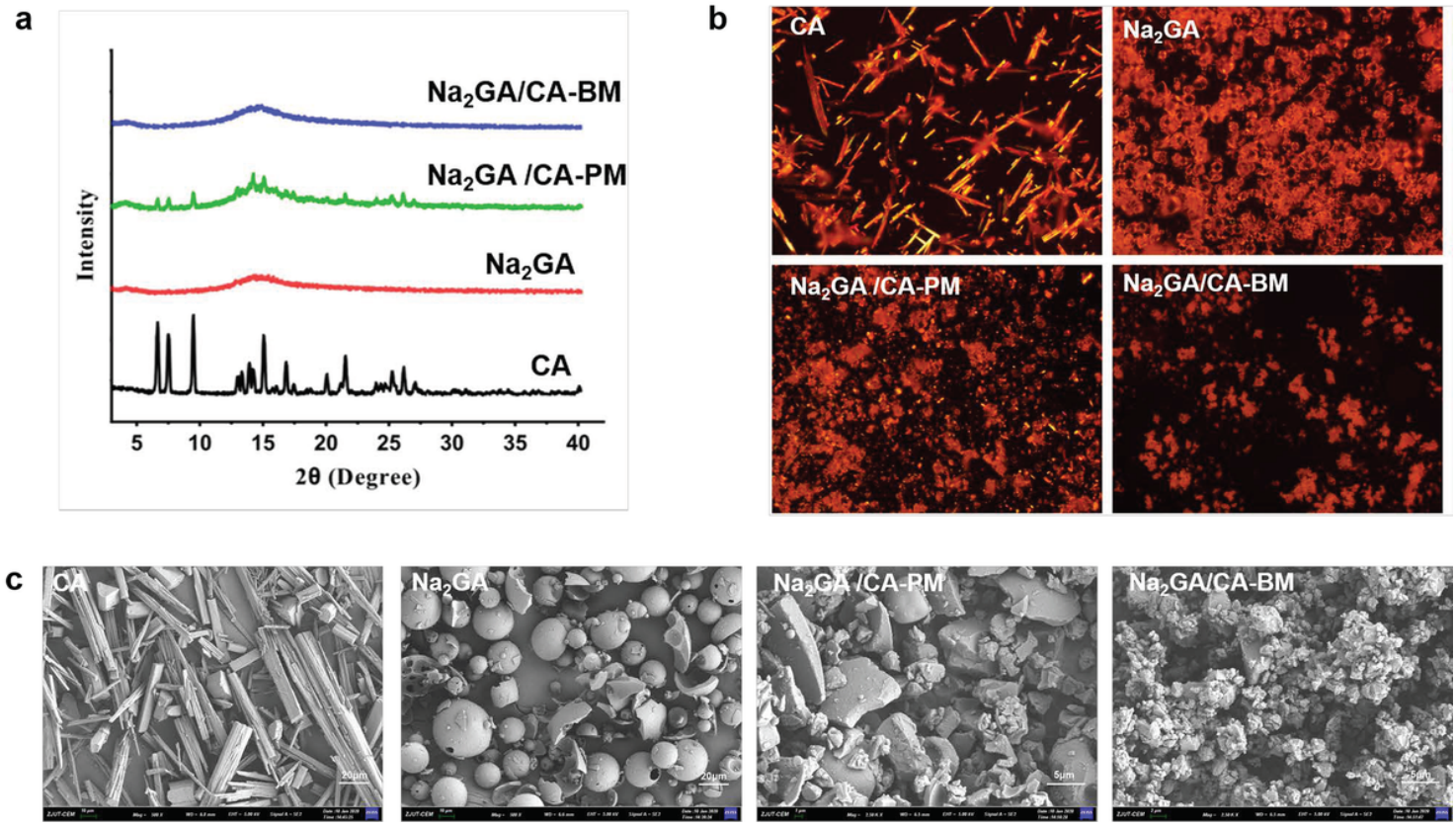

Figure 3

The size, zeta potential and surface morphology of Na2GA/CA-BM. (a) Dynamic light scattering size measurement of Na2GA/CA micelles. (b) Transmission electron micrograph (TEM) of Na2GA/CA micelles, the scale bar from left to right was 500 μm, 200 μm.

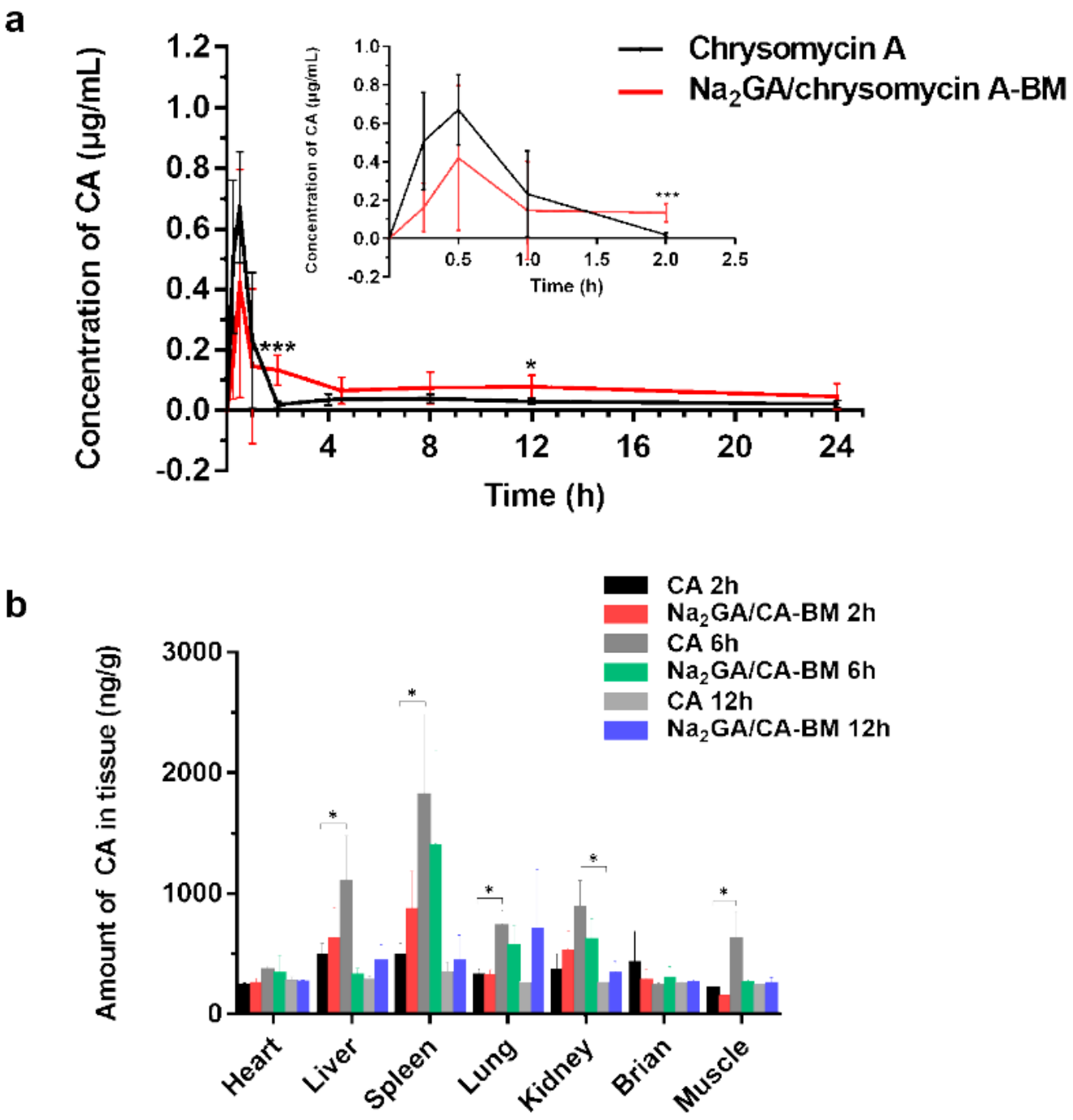

Figure 4

(a) Concentration of CA in ICR mice plasma after intragastric administration of two CA formulations. n =5, *p < 0.05, ***p < 0.001. (b) Biodistribution of chrysomycin A in major tissues of mice after intragastricly administering. n=5, *p < 0.05.

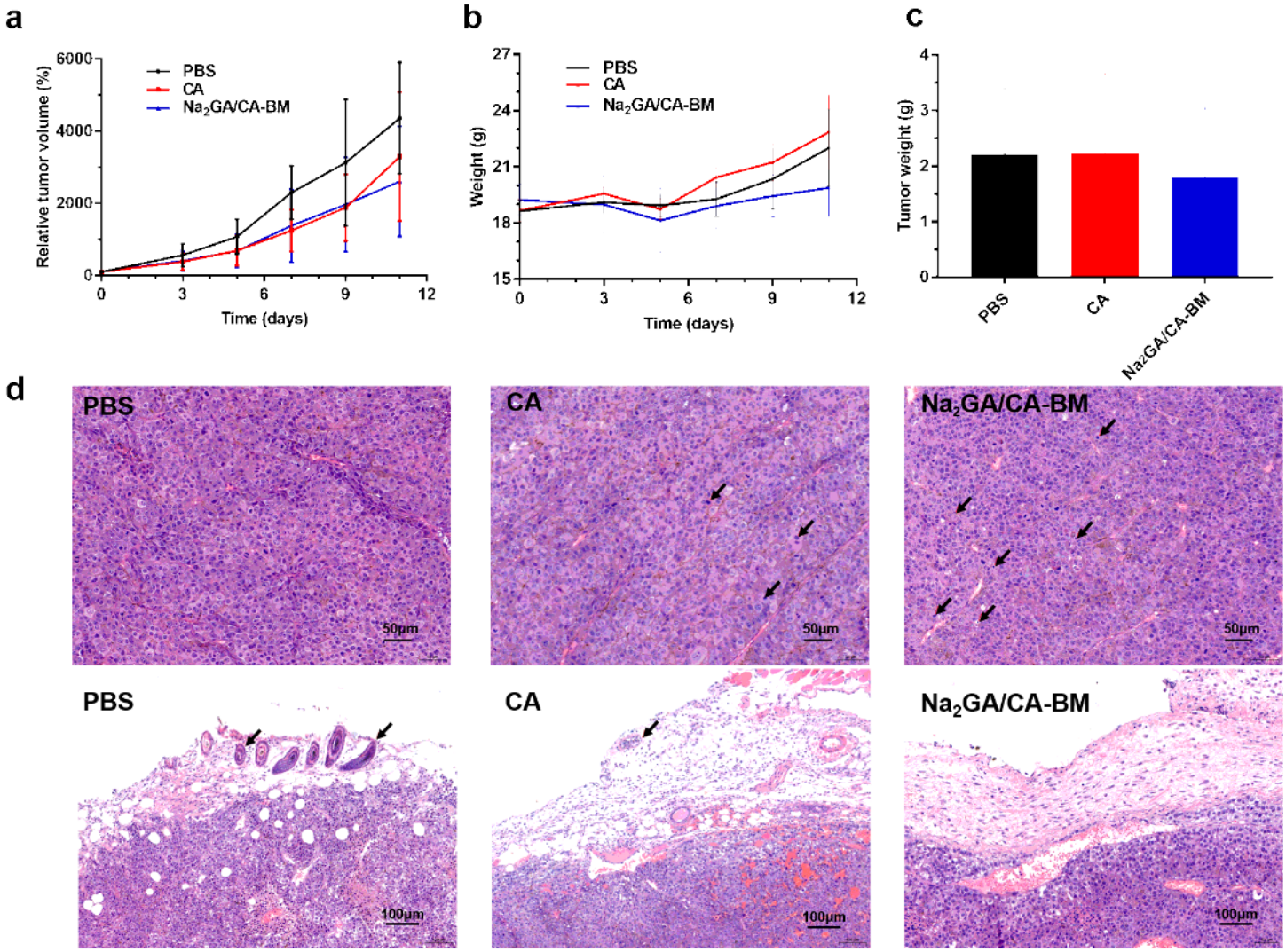

Figure 5

In vivo antitumor effect test in C57BL/6 mice by intragastric administration. (a) The change curve of tumor volume throughout the treatment. (b) The body weight curve of mice. (c) Mean weight of tumor in each group at the end of treatment. (d) H&E staining of tumor tissue sections with envelop layer.

Supplementary Files

This is a list of supplementary files associated with this preprint. Click to download.

- Graphicalabstract.png